Jason Fisk

Superstructural Units in Borate Glasses and Crystals

Abstract

The purpose of this study was to obtain quantitative information on medium range structures in sodium borate glasses through a complementary use of NMR and Raman spectroscopic techniques. This was completed out in the hope of obtaining a calibration factor between the data obtained from the two methods. Sodium borate glasses can be denoted as $xNa_2O(1-x)B_2O_3$, where x is the mole fraction. 30g samples of sodium borate glasses with a range of mole fractions; $0.0 \le x \le 0.67$ were prepared with their structures being deduced from the resultant X-ray diffraction patterns. The crystallisation temperatures of the crystal forming glass samples (x = 0.2, 0.25, 0.33) were determined using differential thermal analysis in preparation of heat treatment resulting in the formation of crystals. NMR and Raman spectroscopy was then performed on both the glass and crystal samples with N_4 values being calculated from the obtained NMR spectra. Peak fitting was attempted on the Raman spectra with the intensities of a range of peaks being integrated to quantify the various amounts of species present. The NMR data displayed a significant lowering of the N_4 fraction in sodium borates with decreasing mole fraction. A calibration of this data was attempted with the NMR data. N_4 values calculated from the intensities of the boroxol ring and surrounding peaks is reported to display a near linear correlation with the N_4 values calculated from NMR for sodium contents in the range 0-25 mol%. The calibration factor is thus; $N_4^{NMR} = (1.5495)\, N_4^{Raman}$.

1. Introduction

The characterisation of crystals can be made by the long range order associated with the position of atoms in the crystal lattice. This means that once the positions of atoms and their neighbours are known at one point, the place of each atom is known precisely throughout the crystal. Glasses however, contain a lack of long range order due to the absence of the underlying periodicity. The presence of short range order is clearly established by X-ray diffraction studies of these materials. This means that the atomic positions cannot be predicted beyond the nearest neighbours of any given atom.

Borate glasses are considered unusual because they contain significant medium range order. It is thought that this is the consequence of the formation of superstructual units in which single

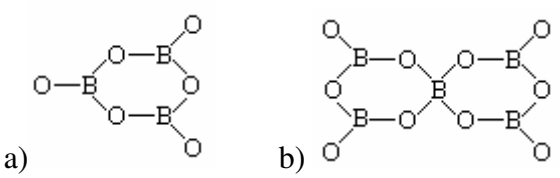

Fig. 1. Two of the superstructual groups present in a borate glass; (a) boroxol group, (b) pentaborate group.

and fused rings are formed from combinations of BO_3 and BO_4 units (Fig.1) .The 3-coordinated (B_3) unit takes the form of a planar triangle and the 4-coordinated (B_4) takes the form of a

tetrahedron. The existence of these structures is a fascinating characteristic of borate glasses and crystals.

Borate glass structures have been extensively investigated by Jan Krogh-Moe, whose theory is by now widely, if not universally accepted. It has been asserted that borate glasses are not merely a random network of BO_3 triangles and BO_4 tetrahedral joined at the corner, but instead they contain well-defined and stable borate groups as segments of the disordered framework. Those borate groups which are included in the glass structure should be identical with groupings which occur in crystalline borates of compositions bordering those of the glasses [2].

Nuclear magnetic resonance has long been used to obtain structural information about glasses, providing a sufficient measure of the fraction of 4-coordinated units within these materials. Raman spectroscopy however, although successful in identifying crystalline arrangements, fails to provide adequate structural information about glasses. This is due to the absence of simplifying symmetry contained within these materials. The task is further hindered by the apparent uncertainty associated with the origin of the peaks produced by this technique, with the analysis made more difficult by the lack of theoretical calculations of vibrational modes of the structural groups in glasses. A clear picture of the effect of disorder is consequently not available.

The objective of this project therefore is to perform a calibration of the data obtained from the two techniques so that N_4 values can be deduced from Raman data by quantifying specific peaks contained within the spectra.

2. Theory of physical techniques

2.1. X-ray Diffraction

X- ray diffraction is a common physical technique in which an atom exposed to a beam of X-rays is a source of a coherent scattered wave, which interferes with those emitted by neighbouring atoms. The method consists of studying the spatial distribution of the total diffracted wave. The arrangement of the crystal structures can be deduced from the diffraction patterns. Here the atoms are in regular planes so sharp X-ray diffraction peaks are observed. If a wavelength; λ, is used to examine a material then for the planes separated by a distance; d, diffraction occurs when the Bragg condition is satisfied:

$$n\lambda = 2d\sin\theta \qquad (1)$$

where the radiation is scattered through an angle 2θ [3].

2.2. Thermal Analysis

Thermal analysis is the measurement of changes in physical properties of a substance as a function of temperature whilst the substance is subjected to a controlled temperature programme.

When a single pure solid substance is heated in an inert atmosphere, the resultant increase in molecular atomic or ionic motion may lead to changes in crystal structure, sintering, melting, or sublimation. If the intramolecular forces are weaker than the intermolecular forces, the substance may decompose forming new molecular fragments, some or all of which may be volatile at the temperatures reached. More complicated reactions result when the initial solid can react with the surrounding atmosphere. When more than one solid substance is present initially, there are correspondingly more possibilities for interaction on heating and new phases, such as solid solutions and eutectic mixtures, may form as well as new compounds formed by addition or double decomposition reactions.

Differential Thermal Analysis (DTA) is the most common and simple thermal analysis technique. Differential thermal analysis involves heating a material at a controlled rate to a pre-determined temperature and comparing any chemical emissions of heat (exothermic) or absorptions of heat (endothermic) from the material in comparison with a reference material. The difference in temperature between the reference material and the sample is recorded whilst both are subjected to the same heating programme [4].

2.3. NMR Spectroscopy

NMR is also a characterization technique where a sample is immersed in a magnetic field and is subjected to a pulse of radio waves. The magnetic moments of the atoms due to their spinning nuclei, within the sample are aligned with the direction of the magnetic field. The radio waves fired at the sample disturbs the magnetic moments of the atoms and orientates them 90 degrees to the direction of the magnetic field. As the moments return to the 'ground state' i.e. inline with the field, they release a burst of energy which is detected. It is the intensity of this energy which is recorded during NMR spectroscopy.

Subatomic particles can be imagined as spinning on their axes. In many atoms these spins are paired against each other, such that the nucleus of the atom has no overall spin. However, when the spins of the protons and neutrons comprising these nuclei are not paired, the overall spin of the charged nucleus generates a magnetic dipole along the spin axis, and the intrinsic magnitude of this dipole is a fundamental nuclear property; the nuclear magnetic moment. The net spin of the nucleus in the case of ^{11}B is 3/2.

Nuclei with a spin number greater than 1/2 have an associated nuclear quadrupole moment. This means that the charge on the nucleus is not spherically symmetrical. As a molecule reorientates itself, there is an interaction between the nuclear spin and the electric field gradient at the nucleus. This provides a mechanism for relaxation, and as a consequence, the spectral lines from quadrupolar nuclei are generally broader than those from spin 1/2 nuclei.

Recently various line narrowing techniques, such as magic angle spinning (MAS) NMR have been developed. This technique produces a reduction of linewidth of more than two orders magnitude in certain crystalline materials, resulting in an increased appreciation of the underlying structural information present in the spectrum [5].

This paper concerns the use of MAS NMR spectroscopy in the analysis of sodium borate structures in both glasses and crystals.

2.4. Raman Spectroscopy

When photons interact with molecules they induce transitions between energy states. Most photons are elastically scattered, a process which is called Rayleigh scattering. In Rayleigh scattering, the emitted photon has the same wavelength as the absorbing photon. However, Raman Spectroscopy is based on the Raman effect, which is the inelastic scattering of photons by molecules.

The Raman effect comprises a very small fraction, about 1 in 10^7, of the incident photons. In Raman scattering, the energies of the incident and scattered photons are different. The energy of the scattered radiation is less than the incident radiation for the Stokes line and the energy of the scattered radiation is more than the incident radiation for the anti-Stokes line. The energy increase or decrease from the excitation is related to the vibrational energy spacing in the ground electronic state of the molecule and therefore the wavenumber of the Stokes and anti-Stokes lines are a direct measure of the vibrational energies of the molecule [6].

3. Experimental procedures

A database search was performed on sodium borate glasses to deduce the range of phases that could be formed from mixtures of varying amounts of sodium carbonate and boric acid. For these phases, the mole fraction, x, was calculated, with repeated values of x being discarded to avoid repetition. The list of phases (with x = 0.05, 0.1, 0.15, 0.2, 0.25, 0.33, 0.5, 0.67) were then used to calculate the relative amounts of sodium carbonate and boric acid needed for a 30g sample of each phase.

3.1. Glass preparation

The sodium carbonate and boric acid compounds were varied in their amounts according to each corresponding phase and carefully weighed using sensitive electronic scales. These scales measured accurately to 3 decimal places producing errors for each batch of approximately ± 0.002g out of each 30 gram sample. 1 mole % of iron oxide was added to each powdered batch to produce better NMR results. The powdered samples were mixed thoroughly on a set of rollers for a period of a 2 -3 hours, finally being poured into a platinum crucible in preparation for the furnace.

All of the samples within the range $0.0 \leq x \leq 0.5$ were heated at 10 ºC/min, to a maximum of 1000 ºC. The molten glasses of each sample were poured into a mould and allowed to set and cool. These rapidly cooled to form translucent glasses using the plate quenching technique. The x = 0.5 sample failed to form into a glass, forming instead into a brown ceramic material. This was reasoned to be because alkali borate glasses with alkali oxide contents of more than 40 mol% lose their ability to form glasses by common quenching techniques. For this reason, the 67 mol% sample underwent a different heating programme. The furnace was allowed to ramp up to 840 ºC at an identical heating rate of 10 ºC/min. It was held at this temperature (which is just below its melting point, deduced from the phase diagram for $Na_2O - B_2O_3$) over a period of 48 hours and allowed to cool at room temperature in an alumina crucible. This formed into a blue tinted white opaque material which had reacted with the alumina crucible towards the edges of the sample.

3.2. X-ray diffraction

Small fragments of each glass were ground up into a fine powder using a pestle and mortar in preparation for X-ray diffraction. The 0.67 sample had to be separated from the crucible with a hammer and was loaded into the X-ray diffraction holder within an argon atmosphere due to the samples high sensitivity to moisture. During the experiment, a film lid was glued onto the holder to again prevent the sample from being exposed to moisture. The angle for each run was set at 0-80º for a period of two or four hours.

3.3. Thermal Analysis

The crystallisation temperatures for the crystal forming sodium borates glasses (x = 0.2, 0.25, 0.33) were deduced using differential thermal analysis. The DTA was programmed to measure the temperature difference between the reference sample and the furnace up to a temperature of 1000 ºC at a rate of 10 ºC/min. The reference material was quartz, and was carefully weighed to match the weight of each sample on electronic scales, giving a difference on average between the two weights as ± 0.001g. This was considered negligible.

The crystallisation peaks were obtained by plotting the differential temperature against the furnace temperature, with the location of the peak being found using the cursor on the graph plotting computer programme. The estimated uncertainty for each crystallisation temperature was ± 5 ºC. This was determined by where the extremes of the peak could conceivably be located.

3.4. The formation and X-ray diffraction of crystals.

The crystal forming glass samples were heat treated in small platinum crucibles at a heating rate of 10 ºC/min up to their respective crystallization temperatures. These formed small crystals, light brown in colour, which were again ground up in preparation for X-ray diffraction. The small powdered batches then underwent X-ray diffraction.

3.5. NMR Spectroscopy

The N_4 values for the glass samples (x = 0.05, 0.1, 0.15, 0.2, 0.25, 0.33) and crystal samples (x = 0.2, 0.25, 0.33) were examined using ^{11}B magic-angle spinning (MAS) NMR at a magnetic field of strength 14.1 T. At this field, MAS experiments yield completely resolved peaks for three and fourfold co-ordinated boron [7]. A small amount of each sample was crushed in air and tightly packed into 4 mm rotors. The spinning rate was 15 kHz. Short pulse durations of 0.7μs in length were used to ensure that all boron sites were homogeneously excited and their integrated peak intensities quantitatively accurate [7]. 1000 scans were averaged with a 1s relaxation delay between scans. It was not possible to perform NMR on the 67 mol% sample due to the inability of packing it into the 4 mm rotors.

The recorded spectra were Fourier transformed and baseline corrected with the N_4 values being evaluated by direct comparison of peak areas, with the error values being taken from the combined errors of discrepancies in peak position. The reference frequency of ^{11}B is 192.04 MHz at this field.

3.6. Raman Spectroscopy

Small flat samples and powdered samples of each glass were used in the following experiment. Raman spectroscopy was performed on the glass samples in the range $0.0 \leq x \leq 0.33$ and on powdered forms of the three crystal samples. 30 acquisitions were deemed sufficient to obtain suitable plots. A 10mW laser was used in the experiment with x50 magnification at room temperature.

4. Results and Discussion

4.1. X-ray diffraction

The diffraction patterns of the samples in the range $0.0 \leq x \leq 0.33$ for the first set of X-ray diffraction experiments showed a few broad peaks which are characteristic of glass structures. An example is shown in figure 2. It was therefore conclusive that glasses had formed.

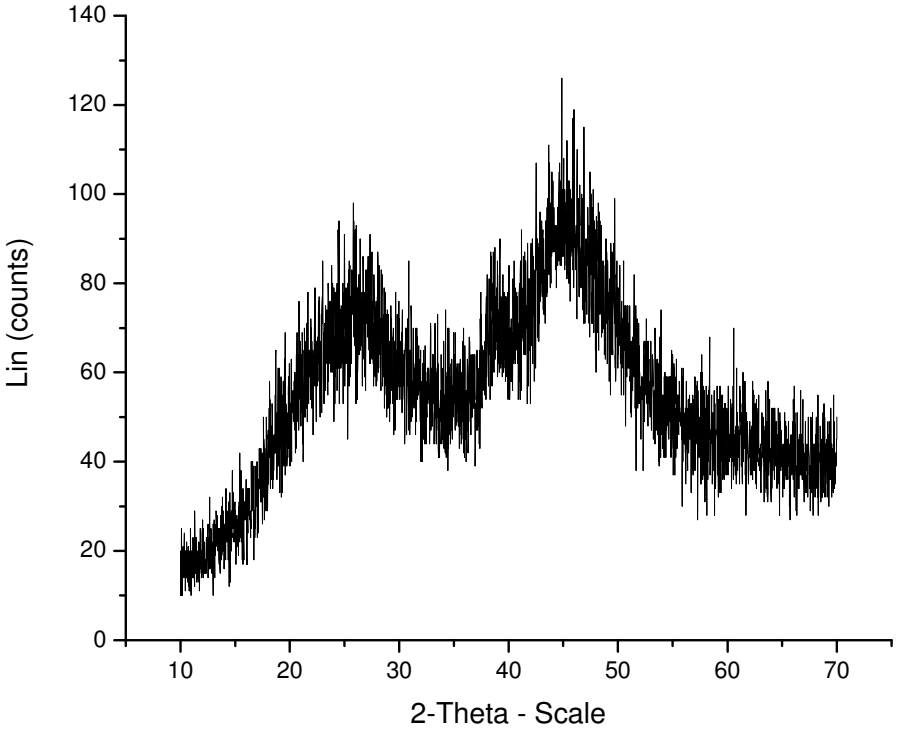

Fig.2. X-ray diffraction pattern for 20 mol% sodium content

The x = 0.5 material had however formed into a crystal. The spectrum of this sample produced distinctive crystalline peaks.

Due to the difficulty of preparing the x = 0.67 sample for X-ray diffraction the experiment was repeated until suitable spectra had been obtained.

The spectra of the crystals in the range $0.0 \leq x \leq 0.5$ were compared with known spectra of sodium borates using the computer database. This was done to ensure that the initial required phases had actually been formed. A difference in phase was observed for the x = 0.5 crystal which is partially due to the high mole fraction of the sample.

The phases of the spectra for the crystals x = 0.2 and 0.25 were comparative to that of known phases for spectra of sodium borates. The discrepancy in the x = 0.33 sample most likely arose from human errors made in the preparation stage of the experiment. A second x = 0.33 crystal was formed for X-ray diffraction but produced similar results. Nonetheless, it was decided that this sample was phase pure enough for NMR and Raman to be performed. The spectra of the x = 0.67 sample is yet to be compared.

4.2. Thermal Analysis

A DTA heating curve is shown in figure 3.

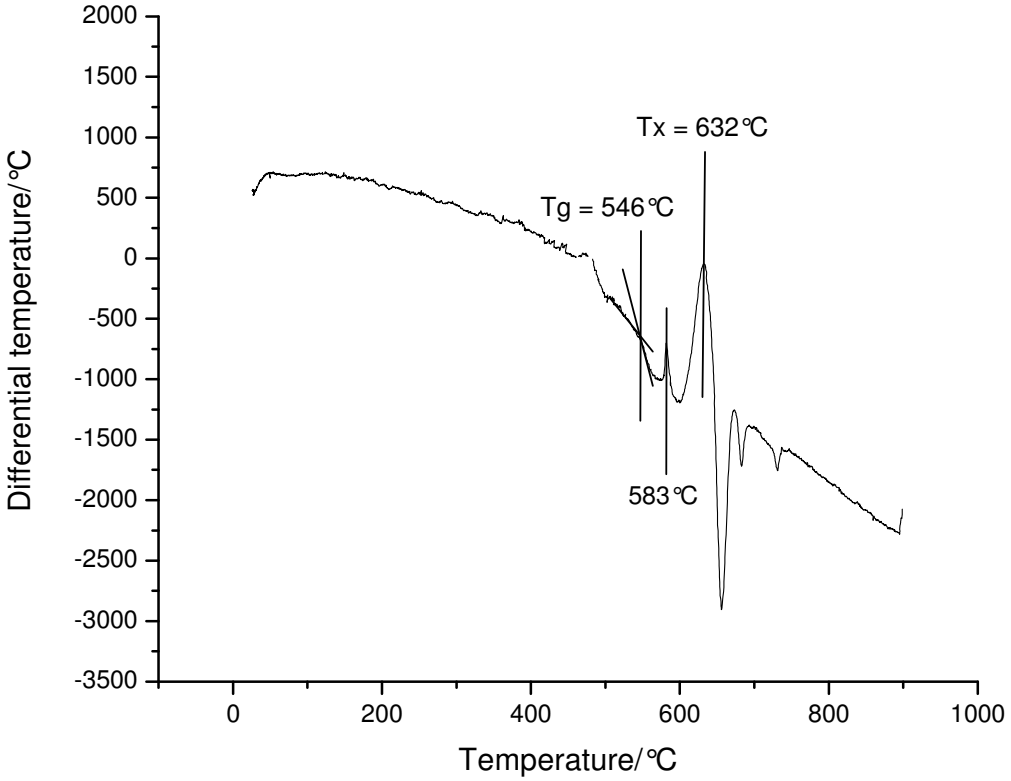

Fig.3. DTA heating curve for x = 0.33 glass showing Tg and Tx temperatures.

The thermal event recorded at 583ºC is a characteristic signature of the quartz reference material.

The measured T_x and T_g values are listed in table 1 for sodium borate glasses in the range $0.0 \le x \le 0.33$.

Glass mol%	T_x/**ºC (± 5 ºC)**	T_g/**ºC (± 5 ºC)**
5		318
10		379
15		421
20	635	472
25	642	491
33	632	546

Table.1. Measured T_x and T_g values for 6 glass samples

The crystallization temperature, T_x, is the temperature at which the sample forms into a crystalline structure. As a material passes through its glass transition temperature, T_g, it's mechanical properties undergo a change from those of a rubber (elastic) to those of a glass (brittle).

4.3. X-ray diffraction for crystal samples; $0.0 \leq x \leq 0.33$

The heat treated glass samples now showed characteristic peaks of crystals in their X-ray diffraction patterns.

4.3. NMR Spectroscopy

NMR produced suitable spectra consisting of peaks corresponding to B_3 and B_4 sites. An example of a spectrum is shown in figure 4.

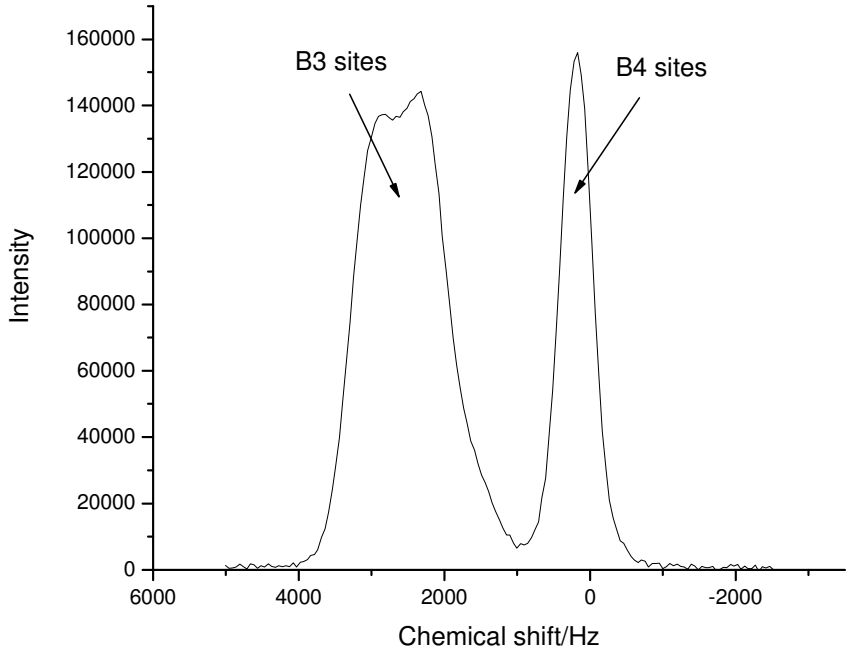

Fig.4. Boron NMR spectra from a sodium borate glass of sodium oxide content 20 mol% showing peaks due to B_3 *and* B_4 *sites*

N_4 values can be calculated using the following equation;

$$\frac{B_4}{B_4 + B_3} \qquad (2)$$

This was done using the integrated intensities of the boron sites of each peak using the tools on the graph plotting computer programme. MAS sidebands which are evident in the acquired NMR spectra originate from the symmetric breathing modes of 3-coordinated boron sites. The presence of these sidebands leads to a 4% correction factor, the effect of which reduces the overall N_4 value. To be completely accurate, the fraction of symmetric 3-coordinated boron sites should be multiplied by 1.04, since this is where the MAS sidebands originate. In practice, however, multiplying the total fraction of 3-coordinated boron sites by 1.04 leads to a more reliable result. This is the method used to produce the corrected fraction of 4-coordinated boron sites. The original and corrected N_4 values are shown in table 2 for both the glass and crystal samples in the range $0.0 \leq x \leq 0.33$. Since the x =

0.5 sample had formed into a crystal, the data obtained from this sample would be impossible to use in any sort of calibration. For this reason no N_4 value is stated for this mole fraction.

Glass mol%	N_4	**Corrected** N_4	**Crystal mol%**	N_4	**Corrected** N_4
5	0.078	0.076			
10	0.150	0.145			
15	0.224	0.217			
20	0.296	0.288	20	0.273	0.264
25	0.377	0.368	25	0.332	0.321
33	0.463	0.454	33	0.461	0.449

Table.2. Original and corrected N_4 values for glasses and crystals in the range $0.0 \le x \le 0.33$

The N_4 values display a significant lowering in value in sodium borate crystals and glasses with decreasing mole fraction over the range studied ($0.0 \le x \le 0.33$). The assertion made by Jan Krogh-Moe [2], stating that the borate groups which are included in the glass structures being identical with groupings which occur in crystalline borates of compositions bordering those of the glasses is also apparent [2]. The fractions for the glasses and crystals with the same mole fraction have similar values. This suggests that similar borate groups exist in both the crystal and glass samples. If this was not the case, then the N_4 value would be different.

4.4. Raman spectroscopy

4.4.1 Glasses

The Raman spectra for six of the sodium borate glasses are shown in figure 5.

The spectrum of the relatively glassy sample (x = 0.05), is characterized by the strong, sharp and highly polarized band at 806 cm^{-1}. The origin of this band has now been widely accepted to be caused by the symmetric ring-breathing vibration of the boroxol ring and can be confidently assigned to this structural unit [9].

The addition of increasing amounts of sodium oxide appears to cause substantial structural changes in the borate network. One of the main effects of increasing x is the rapid decrease of the 806cm^{-1} band intensity, with the simultaneous development of a new band at about 770cm^{-1}. For the glass composition x = 0.25 the 806cm^{-1} feature has disappeared, indicating the absence of boroxol rings, while that at about 765cm^{-1} becomes the dominant Raman band. This feature shifts towards lower frequencies as the sodium content is increased. The Raman band had been previously assigned by Brill [12] to be caused by the symmetric ring breathing vibrations of six-membered ring arrangements containing one or two BO_4 tetrahedra of which pentaborate, triborate and tetraborate units largely represent. However, recent work by Meera and Ramakrishna [13] has suggested that in certain borate glasses, the addition of alkali oxide causes boroxol rings to be converted to pentaborate units alone and not to tetraborate or triborate groups.

In either case, the Raman spectra indicates that the addition of sodium oxide to boron oxide causes the progressive transformation of boroxol rings into pentaborate units, i.e a change of boron coordination number from three to four [9].

Greater structural information was obtained by performing a fitting calculation on the spectra. Gaussian bands were fitted with constraints made on the number and position of the bands where

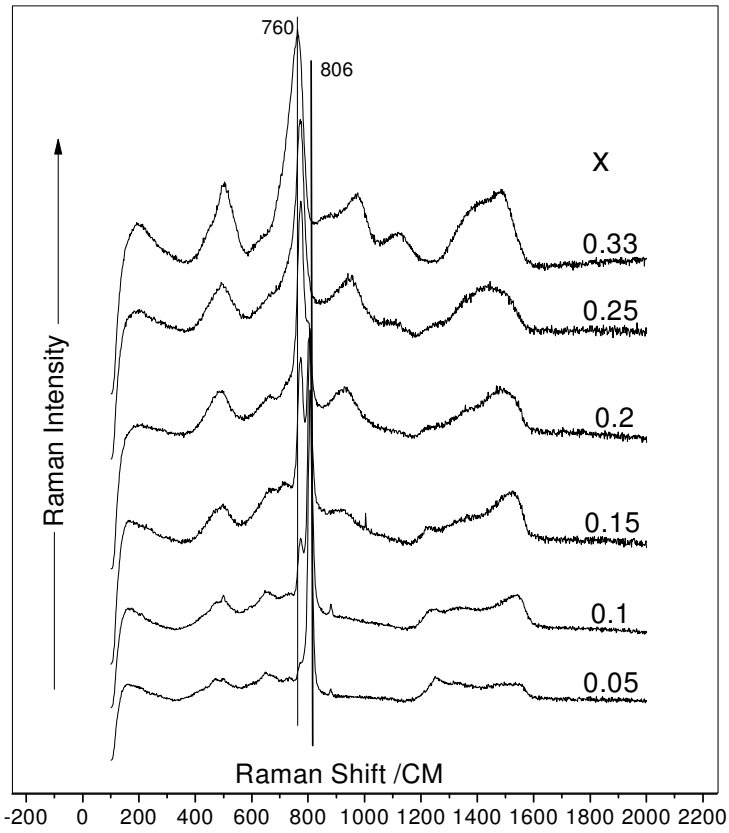

Fig.5. Raman spectra of sodium borate glasses in the composition range $0.0 \leq x \leq 0.33$

identified peaks stated in the literature were known to exist. The best approximation for the background was calculated to be a 2nd order polynomial fit. Experimentally the background of a Raman spectrum is obtained by subtracting the spectrum from a blackbody from that of the sample. This was however deemed impractical due to the obvious lack of availability of a blackbody. All of the spectra were normalised so that the integrated signal intensity was equal to unity. Examples of the peak fits are given in figure 6. The bands were assigned according to literature results as can be seen in table 3.

The medium intensity band (a), located in the region 460-570 cm^{-1} is of considerable interest but as of yet no detailed assignments of this band have been offered. Knowledge of this region however can be obtained by direct comparison with the spectra of crystalline borate compounds reported by Konijnendijk [14]. Using this method, Kamitsos and Karajassides have concluded that the appearance of the envelope around this area originates from contributions by a variety of borate groups including planar six-membered rings with one or two BO_4 tetrahedral and diborate groups [8]. The increase in alkali content has the effect of increasing the peaks intensity.

The band marked (b) in the range 630-690 cm^{-1} is assigned to the breathing modes of the metaborate unit containing one B_3 site with a non-bridging oxygen atom [18]. Its intensity has a maximum for 15 mol% of sodium. The observed trend of the metaborate intensity indicates that if sodium oxide is added above a certain quantity, the presence of BO_3 units from metaborate groups is not favoured any more.

The growing peak (c), located at about 720 cm^{-1} which becomes more dominant for alkali contents above 15 mol% had been argued previously by Brill [15] to be due to the presence of

groups containing two BO_4. However, analysis of crystalline $Na_2O - B_2O_3$ by Meera and Ramakrishna [13] has led to show that this band can in fact be attributed to dipentaborate groups. The intensity of this peak increases over the range $0.0 \leq x \leq 0.33$.

As previously mentioned, the peak labelled (d) is due to pentaborate units, and the peak at (e), which disappears at 25 mol%, represents the boroxol ring.

The asymmetric band envelope (f) at around 950 cm^{-1} has been suggested to arise from vibrations of pentaborate, tetraborate, and connected diborate groups [10]. This peak sharpens over the recorded range.

The weak feature (g) located at about 1100 cm^{-1} can be assigned to interconnected diborate groups [10,11] which become more dominant between 25 and 33 mol%. The effect of increasing the alkali content appears to increasing its intensity.

The band at about 1210 cm^{-1} can be assigned to the symmetric stretching vibrations in pyroborate units [17]. The broad band envelope in the 1300-1600 cm^{-1} region, has been assigned to the stretching of nonbridging $B\text{-}O^-$ bonds attached to large borate segments [11] which typically would be metaborate rings, chain type metaborate units, or triborate groups with one nonbridging oxygen [8]. The peaks representing these structures are not shown in figure 6, but can be seen in the stacked spectra in figure 5.

Borate Group	**Position /cm^{-1}**	**Label**
Six-membered rings with one or two BO_4 tetrahedral and diborate groups	460-570 cm^{-1}	a
Metaborate unit	630-690 cm^{-1}	b
Dipentaborate groups	720 cm^{-1}	c
Pentaborate unit	765cm^{-1}	d
Boroxol ring	806 cm^{-1}	e
Pentaborate/tetraborate/connected diborate groups	950 cm^{-1}	f
Interconnected diborate groups	1100 cm^{-1}	g
Pyroborate units	1210 cm^{-1}	-
Nonbridging $B\text{-}O^-$ bonds attached to large borate segments	1300-1600 cm^{-1}	-

Table.3. Borate groups present in $xNa_2O(1-x)B_2O_3$ *sodium borate glasses in the range* $0.0 \leq x \leq 0.33$

4.4.1 Crystals

The postulation asserted by Jan Krogh-Moe [2] regarding the similarity between borate groups included in glass structures with that of groupings occurring in crystalline borates of compositions bordering those of the glasses is again apparent [2]. The boroxol ring and emerging Raman band [9] are equally evident in the spectra of the crystal samples as are the envelopes located at the 630-690 cm^{-1} and 1300-1600 cm^{-1} regions. A fitting calculation was attempted on the crystalline bands but this proved too difficult due to the complexity of the spectra.

Having assigned the Raman bands to specific borate units, it was now possible to attempt a calibration between this data and the NMR N_4 values.

4.5. Calibration of Raman and NMR data

It was a requirement that the peaks chosen for the calibration showed consistent trends throughout the range 0-33 mol%. It was also invaluable that these peaks displayed a significant increase of B_4 units together with the simultaneous decrease of B_3 units as the alkali content was increased. This would result in the vital increase in N_4 values needed to complete a calibration.

The peak which represented the structural unit of the boroxol ring, the emerging bands containing pentaborate and dipentaborate units [13] at the 750-770 cm^{-1} region, the diborate and pyroborate groups, and the metaborate ring, were investigated for the calibration procedure. These units are represented in figure 7. These bands were chosen because they displayed significant changes in intensity as the alkali content was increased. The peaks which contained 4-coordintaed structures increased in area over the range 0-33 mol% whilst the peaks representing 3-coordintaed structures only, decreased.

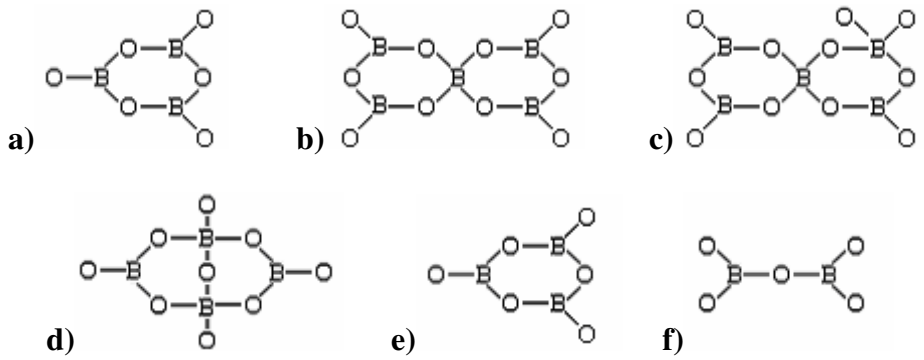

Fig.7. (a) boroxol group, (b) pentaborate group, (c) dipentaborate group, (d) diborate group, (e) metaborate ring, (f) pyroborate unit.

The amounts of each unit contained within the bands could be realized through the results of integrating the intensities of the respective peaks. As mentioned, the areas of the peaks were normalised so that the total spectral area was equal to unity. Table 4 below displays the results of this computation.

	Na content/mol%						
Structural unit	**Structural N4 value**	**5**	**10**	**15**	**20**	**25**	**33**
Dipentaborate	0.4	1.36	4.25	4.31	6.73	11.75	20.40
Penataborate	0.2	8.19	10.89	15.30	22.32	28.15	25.26
Boroxol ring	0	36.37	26.23	14.71	8.58	0	0
Metaborate ring	0	16.45	13.93	19.03	13.89	8.03	2.47
IC diborate groups	0.5	0	0.34	0.33	0.78	2.26	5.69
Pyroborate units	0	4.62	1.47	1.16	0.88	0.88	0

Table.4. Normalised integrated areas for peaks representing boroxol, penataborate and dipentaborate units, the diborate and pyroborate groups, and the metaborate ring in the range 0-33 mol%

A number of combinations of structures were chosen with the overall N_4 value associated with the respective peaks per mass fraction being determined using the following equation;

$$(\sum(N_4^{structural} \times A^{peak}) / A^{total} \qquad (3)$$

where $N_4^{structural}$ represents the structural fraction of 4-coordinated sites, A^{peak} represents the area of the peak, and A^{total} represents the total area of the three peaks.

The best systematic increase in N_4 value was observed when the peaks representing the boroxol ring, and the emerging pentaborate and dipentaborate groups were utilized. The results of this are shown in table 5.

Na content/mol% -	**5**	**10**	**15**	**20**	**25**	**33**
Total area -	45.92	41.36	34.33	37.63	39.89	45.67
Total N4 value -	**0.048**	**0.094**	**0.139**	**0.190**	**0.259**	**0.289**

Table.5. Calculated N_4 values for boroxol ring, pentaborate, and dipentaborate structural units in the range 0-33 mol%

From table 5, an increase in N_4 can be observed up to and including an alkali content of 33 mol%. At 33 mol%, however, the amount the N_4 fraction value is increased by is less than the previous systematic increases for the glasses in the range 0-25 mol%. Work by Meera and Ramakrishna [13] has concluded that at this sodium content, the presence of pentaborate units, which were previously identified by the 770cm^{-1} band, are no longer dominant. Although it is suggested [13] that dipentaborate units still remain present up to an alkali content of 70mol%, the drastic decrease in pentaborate units at about 33 mol% results in the observed decline in systematic increase of N4 value.

A plot of N_4 calculated from the NMR data against the N_4 calculated from the Raman data, shown in figure 8, provides a linear relationship between the two sets of data.

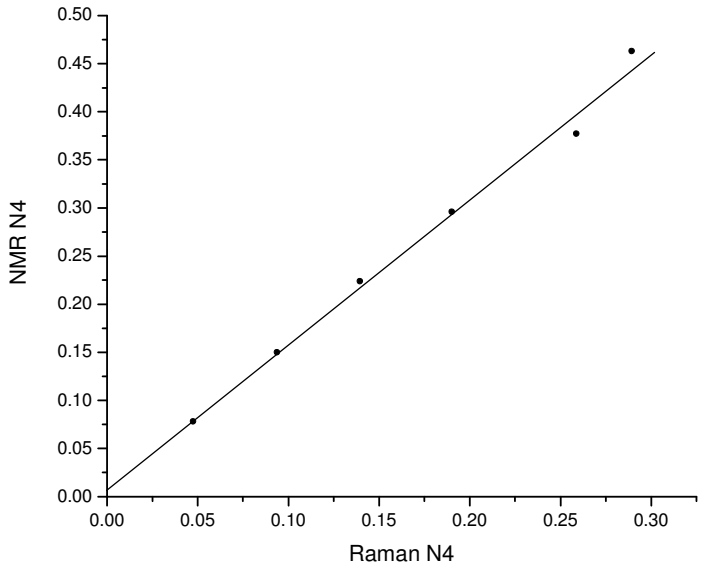

Fig.8. Plot of NMR obtained N_4 values against Raman obtained values N_4

The equation connecting the two sets of data from this relationship is given by;

$$N_4^{NMR} = (1.5153)\, N_4^{Raman} + 0.0073 \qquad (4)$$

where N_4^{NMR} is the N_4 value obtained from the NMR spectra and N_4^{Raman} is obtained from the peaks representing boroxol, pentaborate and dipentaborate units from the Raman spectra.

The N_4 value of a pure glass sample (x = 0) should be zero. It would therefore be logical to force the trend line in figure 8 to pass through the origin. This yields the equation;

$$N_4^{NMR} = (1.5495)\, N_4^{Raman} \qquad (5)$$

It can be postulated that the reason the trend line in figure 8 fails to pass through the origin is due to errors made in the fitting of the individual peaks. Due to the inherent difficulty in precisely locating a number of peaks contained within a single band, errors made in accurately quantifying their respective areas inevitably arises. When combined together to provide an N_4 value for these structures, the deviations in peak area lead to an overall larger error in the fraction of 4-coordianted boron sites. This is the observed result in the above calibration. It can be assertively stated that a more exact peak fitting of these three bands would result in a more confident N_4 fraction value which would be reflected pictorially by the trend line passing closer to the origin. Nonetheless, the trendline in figure 8 would pass through the origin within acceptable error boundaries.

The calibration obtained does provide a procedure for acquiring the fraction of 4-coordinated boron sites solely by using the data produced by Raman spectroscopy for sodium borate glasses in the range 0-33 mol%. A requirement of this procedure is the quantifying of the boroxol ring, and the emerging peaks representing pentaborate and dipentaborate structures. Once the intensities of these peaks have been obtained, one only has to apply equation 5 to this set of data to obtain the N_4 fractions.

5. Conclusion

Although a calibration of sort is reported, gaining accurate N_4 values from Raman data still appears to be a rather unclear procedure. This is mainly due to the apparent ambiguity associated with the origin of peaks obtained thorough Raman spectroscopy. Even though it is possible to assign such peaks, accurately quantifying them to obtain reliable structural information on glasses still proves difficult. The situation becomes more complicated when more than one group gives rise to vibrational peaks in the same region, each of these groups having their own associated N_4 values. The possible combinations of peak positions, areas and widths, contained within these regions are exhaustive. The only way that a reliable attempt can be made to fit these bands is to observe systematic trends over a range of alkali contents, and to manipulate the peak fits to follow these trends as closely as possible. Even this method however can lead to falsity. One way of assigning the peaks more confidently is to compare the spectra of known structures with that of the recorded spectra.

It is accepted that increasing the sodium content leads to a change of boron coordination number of three to four in the range investigated. This is largely observed through the rapid depletion of the boroxol ring with the simultaneous development of bands associated with pentaborate and dipentaborate units [13]. As previously stated, the origin of the latter two peaks still gives rise to an air of doubt. Brill [15] had previously assigned the 770cm^{-1} band to contain triborate, tetraborate, or

pentaborate units and the downshifted band at about 750cm^{-1} to contain diborate, ditriborate or dipentaborate units. Through his study of $Na_2O - B_2O_3$, Konijnendijk [16] had developed a semiquatitative model which suggests that the 770cm^{-1} band is due to tetraborate groups and the down-shifted band at 750cm^{-1} is the result of diborate groups. All of the groups mentioned contain 4-coordianted units, so the assertion that increasing the sodium content leads to a change of boron coordination number still holds even if the peaks are assigned as dictated by conflicting literature allocations.

The reported calibration concerning the boroxol, pentaborate and dipentaborate groups appears to hold for the range of mass fractions investigated. It is doubtful however whether it would still give reliable values for the B_4 fraction beyond 33 mol%. This could be due to the lack of dominance of the pentaborate unit at this point, or the effect of the entirely diminished boroxol ring. Nonetheless, it is difficult to say if this observed lowering in the N_4 fraction is due to these events or whether it has been affected by errors made in the peak fitting calculation of the three peaks for this mass fraction. What is certain is that the reported calibration would begin to fragment after about 45 mol%. Up to this alkali content, the borate network is still well connected through BO_4 bridges. Higher Na_2O contents accelerate its progressive destruction through the formation of B-O$^-$ bonds [8].

6. Future work

Verification of the reported calibration would be paramount to any future work related to this project. This could be performed by analysing the spectra of a different alkali borate such as caesium borate, over the examined concentration range. The Raman peak areas representing the boroxol ring, and the dipenataborate and pentaborate units, would have to be quantified, with the predicted N_4 fractions being realized through the application of equation 5 to this data.

References

[1] Warwick University, Superstructual units in borate glasses and crystals, labscript
[2] L.D. Pye, V.D. Frechette, N.J. Kreidl, Material science research, volume 12, BORATE GLASSES, STRUCTURE, PROPERTIES, APPLICATIONS, Plenum press, 1997
[3] A. Guinier, D. L Dexter, X-ray studies of materials, John Wiley & Sons, New York, 1963.
[4] M. I. Pope, M. D. Judd, Differential Thermal Analysis, pg 1, Heyden & Son Ltd, 1977.
[5] R. Dupree and D. Holland, MAS NMR: a new spectroscopic technique for structure determination in glasses and ceramics.
[6] http://carbon.cudenver.edu/public/chemistry/classes/chem4538/raman.htm.
[7] Jessica R. Berryman *et al,* Thermal, acoustic and nuclear magnetic resonance studies of caesium borate glasses, Journal of non-Crystalline Solids, 2001.
[8] E. I. Kamitsos and M. A. Karakassides, Structural studies of binary and pseudo binary sodium borate glasses of high sodium content, Physics and Chemistry of Glasses, Vol. 30 No. 1, 1989
[9] E. I. Kamitsos and G. D. Chryssikos, Borate glass structure by Raman and infrared spectroscopies, Journal of Molecular Strucuture, 247, 1991
[10] E. I. Kamitsos, M. A. Karakassides and G. D. Chryssikos, *Physics Chem. Glasses*, 28 (5), 203, 1987.
[11] E. I. Kamitsos, M. A. Karakassides and G. D. Chryssikos, *J. Phys Chem*, 1987
[12] T. W. Brill, Philips Res. Rep., Suppl. No. 1 (1975) 1.
[13] B. N. Meera and J. Ramakrishna, Raman spectral studies of Borate Glasses, Journal of Non-crystalline solids 159 (1993) 1-21.
[14] W. L. Konijnedijk, Philips Res. Rep. Suppl. (1975) No. 1.
[15] T. W. Bril, Philips Res. Rep. Suppl. No. 2 (1976) 111.
[16] W. L. Konijnendijk, Philips Res. Rep. Suppl. No. 1 (1975) 243.
[17] S. D. Ross. (1972). Inorganic infrared and Raman spectra. McGraw-Hill, New York. P. 260.
[18] T. W. Brill, (1976). Philipis Res. Rep. Suppl. No. 2.